The description of deformation and destruction of materials containing hydrogen by means of rheological model

Alexander K. Belyaev [a], Natalia R. Kudinova [b,*], Vladimir A. Polyanskiy [a], Yury A. Yakovlev [b]

[a] Peter the Great St. Petersburg Polytechnic University, 29 Politekhnicheskaya St., St. Petersburg 195251, Russian Federation
[b] Institute of Problems of Mechanical Engineering RAS, 61, Bolshoi Pr. V.O., St. Petersburg 199178, Russian Federation

Abstract

The two-continuum rheological model taking account of a change in the hydrogen-binding energy has been proposed in this paper. As in the case of conventional approach our model makes it possible to describe the hydrogen transfer and its accumulation in the metals and to explain changes in the mechanical properties of metals that are caused by that accumulation. The proposed rheological model describes the hydrogen transition from a mobile state to the bound one, depending on the stress–strain state. Concurrent with this achievement our model describes the changes in the material matrix taking place as a result of the hydrogen addition to the matrix atoms. These processes lead to weakening and destruction of the material.

1. Introduction

Taking into account the effect of hydrogen on the mechanical properties of materials is an extremely crucial problem for science and modern practice. The interaction between hydrogen and solid materials is a good mechanical example of the effect of a small parameter. For instance, aluminum alloys with mean hydrogen mass concentrations of 0.4–0.8 ppm (part per million) display hydrogen-induced embrittlement.

Hydrogen embrittlement is the reason for numerous catastrophes, so its mechanisms are thoroughly studied [1–6].

It is impossible to design modern constructions without precise calculations carried out in advance. Since hydrogen strongly affects material strength, there are many studies concentrated on simulating this effect. Several basic approaches have been developed taking into account the effect of hydrogen on dislocation emergence and movement, and on crack formation. Approaches taking into account internal hydrogen pressure in metals and physical approaches have also appeared.

The emergence and movement of dislocations and their effect on localized plasticity (Hydrogen-Enhanced Localized Plasticity (HELP)) near crack tips leads to

---

* Corresponding author.
E-mail addresses: vice.ipme@gmail.com (A.K. Belyaev), natalii@sibmail.com (N.R. Kudinova), vapol@mail.ru (V.A. Polyanskiy), yura.yakovlev@gmail.com (Y.A. Yakovlev).

local plasticity occurring in the materials due to very high dislocation concentrations. The HELP mechanism was first described in Ref. [7]. Later, based on the physical considerations of the interaction potentials between hydrogen and dislocations, Refs. [8–10] formulated the constitutive equations modeling the local changes in material properties at the mouth of a microcrack.

At the same time, the calculations carried out in Ref. [8] indicate that substantial changes in the mechanical properties of a material occur for local hydrogen concentrations of about 9000 ppm, which is a very high value for most metals.

The constitutive equations assume an implicit power-law dependence on local hydrogen concentration that cannot be measured directly, i.e. the parameters of the equations (including the exponent) can be assessed only indirectly. Due to this circumstance, these parameters for specific materials cannot be found experimentally, which may result in significant errors in strength calculations.

To verify the model in Ref. [11], we calculated local plasticity for a crack with a spherical tip. We were able to demonstrate that even model local hydrogen concentrations are only 100 higher than the mean baseline data. Considering these means are commonly values of about 1 ppm, local concentrations do not exceed 100 ppm. Therefore, the test calculation does not confirm that local hydrogen accumulation in metals under external mechanical loads is possible for concentrations up to about 9000 ppm (i.e. steels).

Using modified Fick's law for the HELP model is another source for its possible errors [12]. This law explicitly includes the temperature dependence of the stress pattern coefficients but does not include the exponential dependence of the diffusion coefficient on temperature, which means there is no balance in taking into account the thermal velocities of hydrogen particles and the main matrix of a material. In other words, the effect of the temperature on the matrix is taken into account while its effect on hydrogen particles is not.

There are quite a number of uncertainties described by the authors of the model; in particular, there is a nonlinear dependence of the inner potential on the stress intensity and on hydrogen concentration. Since this model implies dealing with large local concentrations many times higher than those observed in practice, all nonlinearities must play a major role.

There is also the decohesion model (Hydrogen-Enhanced Decohesion (HEDE)) [13] that is similar to HELP. Their difference is that the HEDE model takes into account the decrease in the formation energy of free fracture surfaces that occurs with an increase in local hydrogen concentration.

Ref. [14] notes that the HELP model requires huge computational resources to solve any applied problem, so the only solution is using a continuum model of dislocation evolution. However, this substitute often proves inadequate, which is why the authors recommend using the submicrocrack growth criterion, by which they basically reduce all problems with hydrogen to modeling crack formation and decreasing crack resistance.

The evolution of hydrogen-induced cracks is modeled in Ref. [15]. Initially, it is assumed that the crack has already generated along a pipe's wall, while hydrogen is transformed into a molecular gaseous state and creates excessive pressure contributing to crack growth. The chemical potential gradient depending on stresses is considered to be the main cause of hydrogen diffusion. Additionally, a decrease in crack resistance due to parameter changes of the fracture criterion is taken into account when establishing the conditions for crack growth. Consequently, it is possible to calculate only the crack growth rate that is compared with the experimental results [16].

We should point out that there is no connection between the model and the real physical mechanism of hydrogen effect. Ref. [17] discusses two- and three-dimensional settings of the hydrogen-induced crack growth problem. Significant differences have been found in the values of maximum decohesion stress and threshold stress intensity used for describing metal properties when approximating the same experimental results. As it turns out, these must be set differently. For greater certainty, Ref. [18] recommends selecting these parameters based on only the 3D model.

Ref. [19] presents a theoretical calculation of the changes in the shear modulus and the crystalline lattice parameters of a platinum-zirconium alloy. This calculation was done using wave pseudopotential. The ratio where for each hydrogen atoms there are 3 or 4 matrix atoms (4000 ppm) was used as the calculation basis, which is absolutely improbable for ordinary construction materials. At these hydrogen concentrations hydrides form even in zirconium alloys, i.e., from a mechanical standpoint, the metal turns into a composite.

Ref. [20] takes into account the variation in the stress tensor due to internal pressure that hydrogen creates by penetrating the metal matrix. Tensile tests in samples were simulated by the finite element method (FEM), with the results compared to the experimental data [21]. In contrast with the previous studies, only the effect of hydrogen on the spherical part of the stress tensor was examined. With this approach, the effect of hydrogen is detected only for concentrations above 17 ppm, which, for steels, is a high value (according to the

existing experimental data, e.g., Ref. [33], on average this effect starts at a value that is several times lower).

One more reason to doubt that the comparison of the FEM-calculation results to the data of Ref. [20] was adequate is that the experimental conditions were not described sufficiently. Tensile tests involved grooved samples stretched with simultaneous cathodic hydrogen saturation. Judging from the description of the experiment, hydrogen concentration was not monitored at all. Moreover, the stress-strain curves given in Ref. [20] are performance. Their flaw is that they do not take into account the variations in the diameter of the journal of a sample, which results in underestimating the actual tensile strength and the elastic moduli from the data of these curves.

The molecular dynamics method [22–24] is also used to model hydrogen embrittlement but due to the small sizes of the modeled ensembles this method only allows to describe micromechanisms in crack tips or dislocations, which makes it impossible to model construction behavior. The quantum mechanical approach [25,26] has the same flaw: due to high heterogeneity of real metals it is only applicable to describing crack behavior in perfect crystals or for modeling the behavior of individual microcracks and dislocations.

Thus, to predict the behavior of constructions made of hydrogen-containing materials, a macromodel is necessary that would take into account the effect of small hydrogen concentrations on the mechanical properties of materials.

2. A two-component continuum for modeling hydrogen degradation of materials

Hydrogen is captured into various traps inside materials, such as dislocations, microcracks, surfaces of grains, etc. [1,2]. Each type of trap corresponds to a specific binding energy [27].

The studies of the metal–hydrogen interaction revealed the major role of hydrogen concentration distribution over types of trap or over binding energy levels [28]. For example, the total hydrogen content in steels is 0.2–4.0 ppm. However, only hydrogen with low binding energies (i.e., diffusely mobile) greatly affects strength and plasticity. On the contrary, all of the hydrogen dissolved in aluminum alloys has low binding energies of 0.2–0.8 eV. The diffusely mobile hydrogen concentrations important for mechanical strength have similar values in steels and aluminum alloys, namely, less than 1 ppm. In steels diffusely mobile hydrogen constitutes 5–10% of the total dissolved hydrogen mass. In contrast, all of the hydrogen dissolved in aluminum alloys remains diffusely mobile.

Hydrogen with low binding energies tends to tensile stress zones (the Gorsky effect [29]). The accumulation of hydrogen in a fracture zone can happen both as a result of sorption from the external medium, and of the redistribution of its natural concentrations inside the material. Hydrogen with low binding energies diffuses easily; at the same time, low binding energies indicate that its interaction with metal is very weak. On the contrary, hydrogen with high binding energies interacts very intensely with metal, but migrates very slowly within it. The mechanical properties of the host material deteriorate, mainly due to hard interaction, as hydrogen attached to metal atoms takes energy out of the crystalline structure.

Therefore, an increase in the binding energy of hydrogen is accompanied by the binding energy inside the crystalline lattice decreasing by the same amount, which is associated with a degradation of its mechanical properties [30]. Consequently, the hydrogen-containing material may be assumed to contain two interacting continuums. The diffusely mobile hydrogen mass inside a volume V is written as the following integral:

$$m_H^- = \int\limits_V \rho_H^- dV$$

Here m_H^- and ρ_H^- are the mass and the bulk density of diffusely mobile hydrogen.

The balance equation of hydrogen mass has the differential form

$$\frac{\partial \rho_H^-}{\partial t} + \nabla \cdot (\mathbf{v}_H^- \rho_H^-) = j_H^-,$$

where j_H^- is the bulk source of diffusely mobile hydrogen, $\mathbf{v}_H^-$ is the velocity vector of its movement.

In terms of concentration $N_H^- = \rho_H^-/m_H$ the hydrogen mass balance equation can be written as

$$\frac{\partial N_H^-}{\partial t} + \nabla \cdot (\mathbf{v}_H^- N_H^-) = \frac{j_H^-}{m_H}.$$

A similar mass balance equation can be written for hydrogen bound to the material matrix

$$\frac{\partial N_H^+}{\partial t} + \nabla \cdot (v_H^+ N_H^+) = \frac{j_H^+}{m_H},$$

where N_H^+ and $\mathbf{v}_H^+$ are the particle concentration and velocity of the bound hydrogen particles (and also of the particles of hydrogen-containing material bound to them).

The equality

$$-j_H^- = j_H^+ = j$$

means there is no distributed internal hydrogen transport within the material. Thus, we are describing only the transition of hydrogen from one state to another and its redistribution due to diffusion.

As previously noted, hydrogen concentrations critical for the mechanical properties of the material are, as a rule, rather low. Consequently, the internal transitions of hydrogen particles between energy levels can be described as linear relations:

$$j = \alpha N_H^- - \beta N_H^+. \tag{1}$$

Let us now move on to the dynamic equations of the host material. Rheologically speaking, these are the equations of the first continuum which models the solid body and the hydrogen particles bound to its particles. The dynamic equation of the first continumm has the form

$$\nabla \cdot \tau = (\rho_0 + \rho_H^+)\dot{\mathbf{v}}_H^+ + j\dot{\mathbf{v}}_H^+ + \mathbf{R},$$

where $E\tau$ is the stress tensor, $\mathbf{R}$ is the force of the interaction between the host medium and the diffusely mobile hydrogen (between the continuums).

The second continuum modeling the diffusely mobile hydrogen can evidently be simulated as an ideal gas. The gas pressure p has a positive sign in compression. Therefore, the dynamic equation can be written as

$$-\nabla p = \rho_H^- \dot{v}_H^- - j v_H^- - R.$$

The magnitude of the velocity vector $\mathbf{v}_H^-$ of the diffusely mobile hydrogen particles is small, as this speed describes hydrogen diffusion in a solid body.

The elastic deformation energy of a solid body comprises two parts: the spherical and the deviatoric. We can accordingly identify the spherical part and the inertia tensor deviator

$$\tau = \sigma \mathbf{I} + \mathbf{s},$$

where σ are the principal stresses, $\mathbf{s}$ is the deviator, $\mathbf{I}$ is the unit spherical tensor.

The Gorsky effect means that the triaxial tensile energy determines hydrogen diffusion and the interaction between hydrogen and the host material matrix. Consequently, the spherical part of the stress tensor can be assumed to depend on the second continuum. The dynamic equations of a two-continuum medium in this case have the form

$$\nabla \sigma = (\rho_0 + \rho_H^+)\frac{\partial v_H^+}{\partial t} + j v_H^+ + R - \nabla \cdot s,$$
$$-\nabla p = \rho_H^- \frac{\partial v_H^-}{\partial t} - j v_H^- - R.$$

To simplify further analysis, let us restrict ourselves to a one-dimensional case, as it allows to illustrate the main
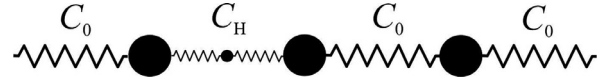

Fig. 1. A one-dimensional model of a crystalline lattice with added hydrogen particles; C_0 and C_H are the hardnesses of elastic bindings in a crystalline lattice without and with hydrogen particles, respectively.

concept of constructing a rheological model of a material containing high natural hydrogen concentrations.

Let us discuss an idealized one-dimensional crystalline lattice of a material. It can be schematically depicted by point masses connected by springs (Fig. 1). The weakening of the interaction between the particles of the material due to hydrogen particles attaching to the crystalline matrix creates a chain of new elastic bindings in the crystalline lattice. These bindings affect the hardness of the whole chain. Evidently, the mass of hydrogen particles can be neglected in this case, i.e., we can assume that $m_0 >> m_H$.

The exact manner of the physical interaction is of no importance for the rheological model. Hydrogen particles may be atoms, molecules or more complex structures, i.e., hydride molecules. The same goes for material particles (and this why we use the term 'particles').

The total chain stiffness taking into account the bulk concentration of hydrogen particles N_0 can be obtained from the following ratio:

$$\frac{N_0}{C_\Xi} = \frac{N_0 - N_H^+}{C_0} + \frac{N_H^+}{C_H}.$$

The constitutive equation, constructed similarly to the one-dimensional model containing added hydrogen particles, has the form

$$\sigma = E_\Xi \varepsilon, \quad E_\Xi = \frac{E_0 E_H N_0}{N_0 E_H + N_H^+(E_0 - E_H)},$$

where σ is the stress; N_0 is the volume concentration of the crystalline lattice particles in an infinitesimal volume; N_H^+ is the volume concentration of the crystalline lattice particles to which hydrogen particles with an elastic constraint C_H have attached (and simultaneously the volume concentration of bound hydrogen); E_H is the equivalent elastic modulus describing the rigidity of the hydrogen-altered binding in the crystalline lattice of the material; E_0 is the initial elastic modulus of the material containing no hydrogen; ε is the strain; E_Ξ is the total elastic modulus of the hydrogen-containing material.

The value of E_Ξ can be significantly lower than the initial elastic modulus of the material containing no hydrogen, as $E_H << E_0$:

$$E_\Xi = E_H \frac{E_0 N_0}{N_0 E_H + N_H^+ E_0} \approx E_H \frac{1}{(N_H^+/N_0)} << E_0. \tag{2}$$

The above equation clearly illustrates the strong effect that the concentration of the attached hydrogen particles N_H^+ has on the total elastic modulus: the higher the proportion of the added hydrogen particles N_H^+/N_0, the lower the elastic modulus of the material.

The number of lattice particles to which hydrogen particles are added depends on lattice stress in each point and on time. The unknown functional relationship between E_Ξ and $N_H^+(\varepsilon, x, t)$ can be found using the two-component continuum model.

The equation for

$$\sigma = \sigma(\varepsilon, N_H^+(\varepsilon, x, t))$$

can be found from Eq. (2) based on the standard form for a one-dimensional elastic chain:

$$\sigma = E_\Xi \varepsilon = E_0 \varepsilon \left[1 - \frac{N_H^+}{N_H^+ + N_0 E_H/(E_0 - E_H)} \right]$$
$$\approx E_0 \varepsilon \left[1 - \frac{N_H^+}{N_H^+ + N_0 E_H/E_0} \right].$$

This equation illustrates the dependence of stresses on the concentration of the added hydrogen particles.

Similarly to the equation for an ideal gas located in the pores and voids of a material, the constitutive equation describing the relationship between the pressure p and the density of the second medium ρ_H^- has the form

$$p = \frac{3}{2} N_H^- kT,$$

where N_H^- is the volume concentration of the mobile hydrogen particles, k is the Boltzmann constant, T is the absolute temperature of the mobile continuum.

We believe that the force R of the interaction between the mobile hydrogen particles and the lattice can be also described through the approach used for ideal gas flow. This allows to obtain the following representation for the quantity R:

$$R = F(\varepsilon)\rho_H^-[v_H^- - v_H^+]. \tag{3}$$

The force of interaction can be regarded as a linear function of the difference between the particle speeds in the two-continuum medium. The parameter $F(\varepsilon)$ (depends on the strain ε) is proportional to the area of the flow section and depends on the properties of the material, such as the parameters of the crystalline lattice, the surface area of crystalline grains, the ratio between this area and the grain volume, porosity, etc.

The source term J was taken in the form suggested in Ref. [31], i.e., similar to Eq. (1):

$$J = \alpha N_H^- - \beta N_H^+,$$

where α and β are the positive coefficients describing sorption and desorption of diffusely mobile hydrogen within the crystalline lattice from diffusion channels.

To illustrate the role of these coefficients, the solution of the equations of particle balance may be used assuming that the volume density distribution of the bound and the mobile hydrogen particles is uniform [31]. This system of equations has the form

$$\begin{aligned} \frac{dN_H^+}{dt} &= \alpha N_H^- - \beta N_H^+ \\ \frac{dN_H^-}{dt} &= -\alpha N_H^- + \beta N_H^+ \end{aligned}. \tag{4}$$

Let us impose the following initial conditions:

$$N_H^+(0) = 0, \qquad N_H^-(0) = \Psi^-.$$

This means that in the initial moment of time there is no bound hydrogen in the material, while the diffusely mobile hydrogen has the concentration Ψ^-. In this case the solutions of the system (4) have the form:

$$N_H^+ = \frac{\alpha}{\alpha + \beta} \Psi^- (1 - e^{-(\alpha+\beta)t}),$$
$$N_H^- = \Psi^- [1 - \frac{\alpha}{\alpha + \beta}(1 - e^{-(\alpha+\beta)t})].$$

The obtained time dependences are shown in Fig. 2. They demonstrate the process of hydrogen saturating the host medium and of the diffusely mobile hydrogen concentration decreasing to equilibrium values determined by the sorption and desorption coefficients. The parameters α and β must be found experimentally, as the sorption and desorption mechanism lie outside the scope of our discussion.

We should note that Eq. (4) describes the exchange of hydrogen particles with different binding energies (the bound and the mobile) on the condition that the mobile hydrogen particles have a zero speed. As follows from Eq. (3), this happens on the condition that $F(\varepsilon) = 0$, i.e. when transfer of mobile hydrogen particles is impossible. Obviously, in this case all diffusely mobile hydrogen is going to change its binding energy and add to the host medium particles on the condition that $\alpha >> \beta$.

After substituting $\rho_H^+ = m_H N_H^+$, $\rho_H^- = m_H N_H^-$ и $n^+ = \frac{N_H^+}{N_0}$ we can write the complete systems of equations for the one-dimensional case of a two-continuum medium in the following form:

$$\begin{aligned} \frac{\partial \sigma}{\partial x} &= (\rho_0 + \rho_H^+)\frac{\partial v_H^+}{\partial t} + Jv_H^+ + R, \\ -\frac{\partial p}{\partial x} &= \rho_H^- \frac{\partial v_H^-}{\partial t} + Jv_H^- - R, \\ \frac{\partial \rho_0}{\partial t} &+ \frac{\partial(\rho_0 v_H^+)}{\partial x} = 0 \\ \frac{\partial N_H^+}{\partial t} &+ \frac{\partial(N_H^+ v_H^+)}{\partial x} = J/m_H \\ \frac{\partial N_H^-}{\partial t} &+ \frac{\partial(N_H^- v_H^-)}{\partial x} = -J/m_H. \end{aligned} \tag{5}$$
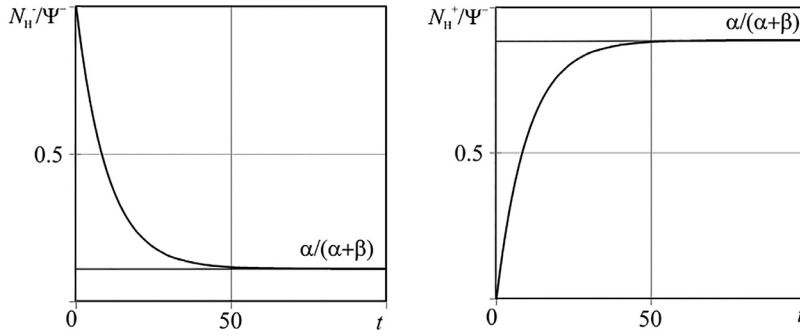
Fig. 2. Plots of normalized concentrations of diffusely mobile (N_H^-) and bound (N_H^+) hydrogen particles versus time for their uniform spatial distribution in the crystalline lattice. Here α and β are the positive coefficients describing sorption and desorption of diffusely mobile hydrogen inside the crystalline lattice, Ψ^- is its initial concentration.

Here

$$\sigma = \frac{E_0 E_H}{E_H + n^+(E_0 - E_H)}\varepsilon,$$
$$R = F(\varepsilon)\rho_H^-[v_H^+ - v_H^-],$$
$$J = \alpha N_H^- - \beta N_H^+.$$

The obtained system of Eq. (5) is complete. At the same time, these equations are strongly non-linear, which is the reason why our further analysis is going to be restricted to the case of static uniaxial stress–strain.

We should note that the concept of a static stress state is rather arbitrary. It must be classified as a balance equation of a continuous medium (5). The assumption of static deformation allows to describe the movement of the second component by pure kinematic relations. In other words, the structural changes in the material over time are a dynamics of sorts. Therefore, it is natural to search for a solution to the problem in the following form:

$$\varepsilon = \varepsilon_{st} + \tilde{\varepsilon}(x,t), \qquad v_H^+ = 0 + \tilde{v}_H^+, \qquad v_H^- = 0 + \tilde{v}_H^-,$$

where ε_{st} is the uniform static deformation.

Evidently, the functional dependence $N_H^+ = N_H^+(x,\varepsilon,t)$ can be represented as

$$N_H^+(x,\varepsilon_{st} + \tilde{\varepsilon},t) = N_H^+(x,\varepsilon_{st},t) + \left.\frac{\partial N_H^+}{\partial\varepsilon}\right|_{\varepsilon=\varepsilon_{st}}\tilde{\varepsilon}(x,t).$$

Respectively, the following equation can be written for the stresses σ:

$$\sigma = \sigma_{st} + \tilde{\sigma} = E_0\left[1 - \frac{n^+}{E_H/E_0 + n^+}\right]\varepsilon_{st}$$
$$+ E_0\left[1 - \frac{n^+}{E_H/E_0 + n^+}\right]\tilde{\varepsilon} + O(\tilde{\varepsilon}).$$

We should note that σ is connected to $\tilde{\varepsilon}$, i.e., there are induced stresses connected to the reorganization of the internal structure that generates the stressses $\tilde{\sigma}$.

The complex relationship of the stress

$$\sigma = \sigma(\varepsilon, N_H^+(\varepsilon,x,t)) = \sigma(\varepsilon, N_0 \cdot n^+(\varepsilon,x,t))$$

and the deformation transform the first equation of the system (5) into the equation

$$\frac{\partial\sigma}{\partial\varepsilon}\frac{\partial\varepsilon}{\partial x} + \frac{\partial\sigma}{\partial n^+}\left[\frac{\partial n^+}{\partial\varepsilon}\frac{\partial\varepsilon}{\partial x} + \frac{\partial n^+}{\partial x}\right]$$
$$= (\rho_0 + \rho_H^+)\frac{\partial v_H^+}{\partial t} + Jv_H^+ + R.$$

Staying within the static approach, we can rewrite this equation as

$$\frac{\partial\sigma_{st}}{\partial\varepsilon}\frac{\partial\varepsilon_{st}}{\partial x} = 0; \tag{6}$$

$$\frac{\partial\tilde{\sigma}}{\partial x} = (\rho_0 + \rho_H^+)\frac{\partial\tilde{v}_H^+}{\partial t} + J|_{\varepsilon=\varepsilon_{st}}\tilde{v}_H^+ + R|_{\varepsilon=\varepsilon_{st}}$$
$$- \left.\frac{\partial\sigma}{\partial n^+}\right|_{\varepsilon=\varepsilon_{st}}\left.\frac{\partial n^+}{\partial x}\right|_{\varepsilon=\varepsilon_{st}}.$$

Here

$$\sigma = E_0\varepsilon_{st}\left\{1 - \left[\frac{n^+}{n^+ + E_H/E_0}\right]\Big|_{\varepsilon=\varepsilon_{st}}\right\},$$
$$\tilde{\sigma} = E_0\tilde{\varepsilon}\left\{1 - \left[\frac{n^+}{n^+ + E_H/E_0}\right]\Big|_{\varepsilon=\varepsilon_{st}}\right\}, \tag{7}$$
$$R|_{\varepsilon=\varepsilon_{st}} = -F(\varepsilon_{st})\rho_H^- v_H^-$$

The second equation in the system (6) describes the dependence of stress pattern $\tilde{\varepsilon}$ induced by bond restructuring, for the case when the principal term is known

$$\left.\frac{\partial\sigma}{\partial n^+}\cdot\frac{\partial n^+}{\partial x}\right|_{\varepsilon=\varepsilon_{st}}.$$

We can write the following relations for the second continuum:

$$-\frac{\partial p}{\partial x} = F(\varepsilon_{st})m_H N_H^- v_H^-, \qquad p = \frac{3}{2}N_H^- kT., \tag{8}$$

where $\rho_H^- = m_H \cdot N_H^-$ is the diffusely mobile hydrogen density.

The Eq. (8) are converted to a form

$$\frac{3}{2}kT\frac{\partial N_H^-}{\partial x} = -F(\varepsilon_{st})m_H N_H^- v_H^-.$$

The last equation is similar to Darcy's law where the diffusion coefficient depends on the strain field ε_{st}.

Therefore, we obtain the following expression for the hydrogen particle speeds (the second continuum)

$$v_H^- = -\frac{3kT}{2F(\varepsilon_{st})m_H}\frac{1}{N_H^-}\frac{\partial N_H^-}{\partial x}. \qquad (9)$$

The above-listed equations should be complemented with the the balance equations for the bound and the diffusely mobile hydrogen particles:

$$N_0\frac{\partial n^+}{\partial t} = \alpha N_H^- - \beta N_0 n^+$$
$$\frac{\partial N_H^-}{\partial t} + \frac{\partial N_H^- v_H^-}{\partial x} = -(\alpha N_H^- - \beta N_0 n^+).$$

Using Eq. (9), we obtain from these equations a new equation for the proprotion of the bound hydrogen particles in the material:

$$\frac{\partial^2 n^+}{\partial t^2} + (\alpha + \beta)\frac{\partial n^+}{\partial t}$$
$$- \frac{3kT}{2m_H F(\varepsilon_{st})}\left[\beta\frac{\partial^2 n^+}{\partial x^2} + \frac{\partial^3 n^+}{\partial t \partial x^2}\right] = 0. \qquad (10)$$

Eq. (10) is a mixed-type equation, as it contains terms typical for hyperbolic equations: $\partial^2 n^+/\partial t^2$, $\partial^2 n^+/\partial x^2$, as well as terms typical for parabolic equations: $\partial n^+/\partial t$, $\partial^3 n^+/\partial t \partial x^2$. This means that a comprehensive analysis of a non-stationary task for a finite initial distrubance must reveal a characteristic moving front of an increase (or a decrease) in hydrogen particle concentration.

In order to analyze this equation, we shall use the Fourier method of variable separation. For this end, we are going to assume that

$$n^+(t, x) = T_+(t) \cdot X_+(x).$$

Then

$$\frac{\ddot{T}_+(t) + (\alpha + \beta)\dot{T}_+(t)}{\frac{3kT}{2m_H F(\varepsilon_{st})}(\beta T_+(t) + \dot{T}_+(t))} = \frac{X''_+(x)}{X_+(x)} = -\gamma_x^2.$$

Hence, we obtain an ordinary differential equation for $X_+(x)$:

$$X''_+(x) + \gamma_x^2 X_+(x) = 0,$$

and also an ordinary differential equation for $T_+(t)$:

$$\ddot{T}_+(t) + \left(\alpha + \beta + \gamma_x^2\frac{3kT}{2m_H F(\varepsilon_{st})}\right)\dot{T}_+(t)$$
$$+ \gamma_x^2\frac{3kT}{2m_H F(\varepsilon_{st})}\beta T_+(t) = 0.$$

Let us solve this problem with the following initial conditions:

$$n^+(0, x) = 0,$$
$$N_H^-(0, x) = \Psi^-\left(1 + cos\frac{2\pi x}{\lambda}\right),$$
$$\dot{n}^+(0, x) = \frac{\alpha\Psi^-}{N_0}\left(1 + cos\frac{2\pi x}{\lambda}\right), \qquad (11)$$

where the parameter λ is determined by the microstructural parameters of the material in question.

First let us construct the equations for the constant term of the $X_+(x)$ series based on the initial conditions (11). In this case $\gamma_x^2 = 0$ and the equation for the time multiplier $T_+(t)$ has the form:

$$\ddot{T}_+(t) + (\alpha + \beta)\dot{T}_+(t) = 0.$$

The solutions of this equation will be the functions of the form

$$T_+(t) = T_0 + T_1 e^{-(\alpha+\beta)t},$$

where the constants T_0 and T_1 are determined by the initial conditions.

For the second term of the $X_+(x)$ series we have the $\gamma_x^2 = \frac{4\pi^2}{\lambda^2}$ value, and the equation for $T_+(t)$ has the form

$$\ddot{T}_+(t) + \left(\alpha + \beta + \frac{4\pi^2}{\lambda^2}\frac{3kT}{2m_H F(\varepsilon_{st})}\right)\dot{T}_+(t)$$
$$+ \frac{4\pi^2}{\lambda^2}\frac{3kT}{2m_H F(\varepsilon_{st})}\beta T_+(t) = 0. \qquad (12)$$

Let us introduce the notation

$$G(\varepsilon_{st}) = \frac{3kT}{2m_H F(\varepsilon_{st})}\left(\frac{2\pi}{\lambda}\right)^2.$$

Then Eq. (12) takes the form

$$\ddot{T}_+(t) + (\alpha + \beta + G(\varepsilon_{st}))\dot{T}_+(t) + G(\varepsilon_{st})\beta T_+(t) = 0.$$

Its solution is a function

$$T_+(t) = T_3 e^{-\xi_1 t} + T_4 e^{-\xi_2 t},$$

where

$$\xi_1 = \frac{1}{2}\left[\alpha + \beta + G(\varepsilon_{st})\right.$$
$$\left. -\sqrt{(\alpha + \beta + G(\varepsilon_{st}))^2 - 4\beta G(\varepsilon_{st})}\right];$$

$$\xi_2 = \frac{1}{2}\left[\alpha + \beta + G(\varepsilon_{st})\right.$$
$$\left. +\sqrt{(\alpha + \beta + G(\varepsilon_{st}))^2 - 4\beta G(\varepsilon_{st})}\right].$$

Substitution into the initial conditions produces, after integration over a full harmonic period, the following relations:

$$T_0 = -T_1 = \frac{\alpha \Psi^-}{N_0(\alpha+\beta)})$$
$$T_3 = -T_4 = \frac{\alpha \Psi^-}{N_0\sqrt{(\alpha+\beta-G(\varepsilon_{st}))^2+4\beta G(\varepsilon_{st})}}.$$

These expressions allow to write the final form of the solution for the relative proportion of bound hydrogen particles:

$$n^+(t,x) = \frac{\alpha \Psi^-}{N_0}\left(\frac{(1-e^{-(\alpha+\beta)t})}{\alpha+\beta} \right.$$
$$\left. + \frac{(e^{-\xi_1 t}-e^{-\xi_2 t})cos\frac{2\pi x}{\lambda}}{\sqrt{(\alpha+\beta+G(\varepsilon_{st}))^2-4\beta G(\varepsilon_{st})}} \right). \quad (13)$$

Predictably, the diffusely mobile hydrogen that is uniformly distributed over the volume increases its binding energy independent of diffusion, while the non-uniformly distributed hydrogen diffuses, with the diffusion rate determined by the function $F(\varepsilon_{st})$ that is a conventional size of the flow section of the hydrogen diffusion channels depending on the strain ε_{st}.

A decrease in the value of $F(\varepsilon_{st})$ leads to an increase in $G(\varepsilon_{st})$. If $F(\varepsilon_{st}) \rightarrow 0$, then ξ_1 will tend to 0, while the multiplier $(e^{-\xi_1 t}-e^{-\xi_2 t})$ in Eq. (13) will tend to $e^{-\beta t}$. These difference between the exponents determines the non-uniformity in hydrogen concentration distribution along the spatial coordinate. Therefore, a redistribution of hydrogen concentrations due to diffusion will decelerate. In the limiting case we will obtain the following formula:

$$n^+(t,x) = \frac{\alpha \Psi^-}{N_0}\left(\frac{1}{\alpha+\beta} + \frac{e^{-\beta t}}{G(\varepsilon_{st})}cos\frac{2\pi x}{\lambda} \right).$$

This means that the redistribution of hydrogen particles in the limiting case will also be determined by the sorption and desorption processes.

The equations of the system (7) can be used to model the effect of hydrogen on the $\sigma(\varepsilon)$ dependence, which is easily measured. We should note that the effects connected to the changes in temperature, and also non-linear phenomena caused by the changes in the bound hydrogen contents due to material deformation can be described by the suggested model.

The experimental data of Ref. [32] prove that the yield point is particularly strongly dependent on hydrogen concentration.

A linearly elastic material may be logically assumed to have a free surface area that, for small strains, is proportional to the deformation itself. Consequently, the α and β coefficients must linearly depend on deformation. Then for small deformations we may adopt a linear dependence for the coefficient ratio:

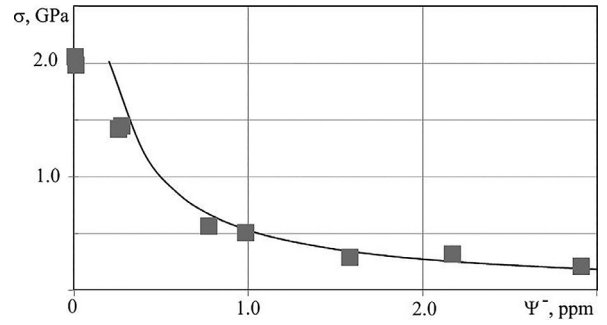$$\frac{\beta}{\alpha} = k_0 + k_1 \varepsilon. \quad (14)$$

Fig. 3. The calculated (line) and the experimental (symbols) values of the maximum tensile stresses in the AISI 4135 steel alloy depending on the initial concnetration of the diffusely mobile hydrogen; the calculation was made using the proposed rheological model; the experimental data is taken from Ref. [33].

The latter relationship depends the change in the material properties during hydrogen redistribution in it, allowing to obtain a good approximation of the experimental data. Fig. 3 shows the dependence of the maximum tensile stresses on the initial diffusely mobile hydrogen concentration for steel. The calculated dependence was compared to the experimental data. This data was obtained in Ref. [33] for the AISI 4135 steel and is represented by the squares in Fig. 3.

The proposed approach was used to study the effect of hydrogen on pipeline wall stresses [34] and on fatigue strength of metals [35,36].

3. Discussion of the results

The discrepancy between the theoretical and the experimental data (see Fig. 3) observed for a low initial concentration of diffusely mobile hydrogen can be attributed to the fracture mechanisms that are not connected to hydrogen effect and, consequently, not described by the model. The rest of the experimental points show a good agreement with the curve, which proves that the model is adequate for describing the examined processes.

As this model describes material fracture, it does not make any assumptions about microcracks existing in the material or of a specific concentration or orientation of dislocations [8]. This approach is also different from modeling hydrogen embrittlement by introducing a crack resistance parameter [15].

According to extensive experimental studies conducted over many decades, the unusually strong effect of hydrogen on the stress–strain behavior of materials can be explained only by the fact that it accumulates in microlocations such as cracks or dislocations. Any attempts to describe such a mechanism by HELP or HEDE

models result in having to simultaneously deal with processes of different scales. In this case, the process at the microlevel often turns out to be localized in the material and temporally unstable. For this reason, certain averaged characteristics have to introduced for calculations of real constructions and numerical modeling (and thus the local peculiarities are found to be diffused) that deprive these models of their initial physical clarity.

The HELP model [7] used a physical mechanism of hydrogen effect that manifests itself as changes in the local mechanical properties of a metal but only for quantitative ratios of about 1 : 1 between hydrogen particles and metal atoms. It proves impossible to obtain these mean hydrogen concentrations to find the specific parameter values of the constitutive equation, and to subsequently set an experiment or carry out a calculation based on the physical mechanisms of the interaction between hydrogen and metal. Such an experiment or a calculation is actually hard to imagine from a physical standpoint, as solid-state hydrogen has a lattice constant that is 1.5 times higher than the corresponding value for most metals.

Therefore, the volume concentration of pure hydrogen particles is even in the solid state three times lower than that of metal atoms.

The main advantage of the proposed constitutive equations and two-component model equations is that they can be applied at a macrolevel. The micromechanisms of hydrogen effect were included into the rheological model. The parameters α, β, E_H, k_0 and k_1 must be determined within the scope of macrovalues, such as experimental stress–strain state diagrams.

Despite the perceived simplicity of this approach and the large number of published data, not all of it can be used for the approximaion in question. Almost all of the experimental data was obtained for samples saturated either in electrolyte solutions or in gaseous hydrogen.

Contrary to the established opinion that hydrogen particles within metals are redistributed rapidly due to the concentration gradient, a simple calculation shows that such a process can last anywhere from tens of hours to several years, and its rate depends on the binding energy of trapped hydrogen. Our own experiments show that in case of zinc hydrogenation through a galvanic process hydrogen concentration redistribution does not become uniform even after a whole year of sample exposure at room temperature.

Therefore, hydrogen concentrations in materials and its volume distributions must be determined accurately in order to find the characteristics of a rheological model. This involves certain difficulties, and the majority of the researchers find these parameters indirectly by measuring cathodic current and charging time. As a result, the obtained data is unsuitable for determining model parameters, as hydrogen is in this case located near sample surface. For example, there is as yet no unique relationship established between ultimate tensile strength and hydrogen-charging time [37].

A descending part present on the $\sigma(\varepsilon)$ curve of a hydrogen-containing material indicates the instability of the material under stress. The failure under an actual load will occur when the point of the maximum stress is reached in the respective curve. This point can be interpreted as the ultimate tensile strength of the material due to its hydrogen saturation.

4. Conclusions

The proposed model allows to describe the kinetics of hydrogen particles in metals, and, in particular, to assess the transition of hydrogen from a mobile to a bound state (depending on the stress–strain state of the material) and to describe the accumulation of bound hydrogen which ultimately leads to material fracture.

Using the model does not require making any presumptions of defects and their distribution in the material.

Analyzing the linear, as well as non-linear model approximation for the case of uniaxial tension in the absence of hydrogen diffusion, produces adequate results.

We suggest a new approach to simulating the behavior of deformed solid matter taking into account the effect of hydrogen on free surfaces and interatomic bonds in single crystals on different scales. This gives grounds for applying the model to describing multi-scale materials with nano- and microstructures.

Acknowledgment

References

[1] P.V. Geld, R.A. Ryabov, L.P. Mokhracheva, Vodorod i fizicheskiye svoystva metallov i splavov [Hydrogen and Physical Properties of Metals and Alloys], Nauka, Glavnaya redaktsiya fiziko-matematicheskoy literatury, Moscow, 1985.

[2] B.A. Kolachev, Vodorodnaya khrupkost metallov [Hydrogen Embrittlement of Metals], Metallurgiya, Moscow, 1985.

[3] J.P. Hirth, Effects of hydrogen on the properties of iron and steel, Metall. Mater. Trans. A 11 (1980) 861–890.

[4] M. Nagumo, Function of hydrogen in embrittlement of high-strength steels, ISIJ Int. 41 (6) (2001) 590–598.

[5] R.J. Bourcierf, D.A. Koss, Hydrogen embrittlement of titanium sheet under multiaxial states of stress, Acta Metall. 32 (11) (1984) 2091–2099.

[6] G.M. Bound, I.M. Robertson, H.K. Birnbaum, The influence of hydrogen on deformation and fracture processes in high-strength aluminum alloys, Acta Metall. 35 (9) (1987) 2289–2296.

[7] H.K. Birnbaum, P. Sofronis, Hydrogen-enhanced localized plasticity—a mechanism for hydrogen-related fracture, Mater. Sci. Eng. A 1–2 (31) (1994) 191–202.

[8] P. Sofronis, Y. Liang, N. Aravas, Hydrogen induced shear localization of the plastic flow in metals and alloys, Eur. J. Mech. A/Solids 6 (2001) 857–872.

[9] D. Delafosse, T. Magnin, Interfaces in stress corrosion cracking: A case study in duplex stainless steels 1998, Solid State Phenom. 59–60 (1998) 221.

[10] D. Delafosse, T Magnin, Hydrogen induced plasticity in stress corrosion cracking of engineering systems, Eng. Fract. Mech. 6 (2001) 693–729.

[11] A. Taha, P. Sofronis, A micromechanics approach to the study of hydrogen transport and embrittlement, Eng. Fract. Mech. 6 (2001) 803–837.

[12] H.P. Van Leeuwen, The kinetics of hydrogen embrittlement: A quantitative diffusion model, Eng. Fract. Mech. 1 (1974) 141–161.

[13] A.G. Varias, A.R. Massih, Simulation of hydrogen embrittlement in zirconium alloys under stress and temperature gradients, J. Nucl. Mater. 2–3 (2000) 273–285.

[14] A.V. Ignatenko, I.K. Pokhodnya, A.P. Paltsevich, V.S. Sinyuk, Dislocation model of hydrogen-enhanced localizing of plasticity in metals with BCC latttice, Paton Weld. J. 3 (2012) 15–19.

[15] A. Traidia, M. Alfano, G. Lubineau, S. Duval, A. Sherik, An effective finite element model for the prediction of hydrogen induced cracking in steel pipelines, Int. J. Hydrog. Energy 21 (2012) 16214–16230.

[16] R.C. Brouwer, D. Ritchie, Modelling hydrogen-induced crack growth: Validation by comparison with experiment, in: Proceedings of the 1995 Conference on Corrosion and Infrastructure–Extended Abstracts, Baltimore, Maryland, November 28–30, 1995, p. 70.

[17] A. Alvaro, V. Olden, O.M. Akselsen, 3D cohesive modelling of hydrogen embrittlement in the heat affected zone of an X70 pipeline steel, Int. J. Hydrog. Energy 18 (2013) 7539–7549.

[18] A. Alvaro, V. Olden, O.M. Akselsen, 3D cohesive modelling of hydrogen embrittlement in the heat affected zone of an X70 pipeline steel – Part II, Int. J. Hydrog. Energy 7 (2014) 3528–3541.

[19] Y. Pan, W. Guan, M. W., J. Zhang, Ch. Wang, Zh. Tan, Hydrogen embrittlement of Pt$_3$Zr compound from first-principles, J. Alloys Compd. 585 (2014) 549–554.

[20] J.P. Carrasco, N. Cesar dos Santos, A.A. Silv, Numerical simulation of the hydrogen effect on the deformations of test body models loaded under tensile stress, Int. J. Model. Simul. Pet. Ind. 1 (2007) 55–62.

[21] G.P. Tiwari, A. Bose, J.K. Chakravartty, S.L. Wadekar, M.K. Totlani, R.N. Arya, R.K. Fotedar, A study of internal hydrogen embrittlement of steels, Mater. Sci. Eng. 2 (2000) 269–281.

[22] Z. Hu, S. Fukuyama, K. Yokogawa, S. Okamoto, Hydrogen embrittlement of a single crystal of iron on a nanometre scale at a crack tip by molecular dynamics, Model. Simul. Mater. Sci. Eng. 4 (1999) 541–551.

[23] M. Wen, X.-J. Xu, Y. Omura, S. Fukuyama, K. Yokogawa, Modeling of hydrogen embrittlement in single crystal Ni, Comput. Mater. Sci. 30 (3–4) (2004) 202–211.

[24] J. Song, W.A. Curtin, A nanoscale mechanism of hydrogen embrittlement in metals, Acta Mater. 4 (2011) 1557–1569.

[25] S. Serebrinsky, E.A. Carter, M. Ortiz, A quantum-mechanically informed continuum model of hydrogen embrittlement, J. Mech. Phys. Solids 10 (2004) 2403–2430.

[26] S. Murray Daw, M.I. Baskes, Semiempirical quantum mechanical calculation of hydrogen embrittlement in metals, Phys. Rev. Lett. 17 (1983) 1285–1288.

[27] G. Pressouyre, A classification of hydrogen traps in steel, Metall. Trans. A 10 (10) (1979) 1571–1573.

[28] A.M. Polyanskiy, V.A. Polyanskiy, Yu.A. Yakovlev, Issledovaniye ppotsessov ustalosti i pazpusheniya metallicheskikh matepialov s ppivlecheniyem metoda oppedeleniya enepgii svyazi vodoroda v tverdom tele [Investigation of the processes of fatigue and destruction of metal by method for determining of the binding energy of hydrogen in solid], Deformatsiya i razrusheniye materialov № 3 (2009) 39–43.

[29] W.S. Gorsky, Theorie des elastichen Nachwirkung in ungeordneten Mischkristallen (elastische Narchwirkung zweiter Art), Phys. Zeitschrift der Sowjetunion 8 (1935) 457–471.

[30] A.M. Polyanskiy, V.A. Polyanskiy, Sposob opredeleniya modulya uprugosti materiala s kristallicheskoy strukturoy [Method of determining the modulus of elasticity of the material with the crystal structure], Pat. № 2366921 RF, MPK G01N 3/00. zayavka № 2008116518/28; Zayavlena 18.04.08; Opublikovano 10.09.2009 Byul.№25.

[31] D. Indeitsev, B. Semenov, About a model of structural-phase transformations under hydrogen inuence, Acta Mech. 195 (2008) 295–304.

[32] E. Lunarska, Z. Wokulski, Effect of hydrogen charging on stress-strain curves for iron whiskers, Acta Metall. 30 (1982) 2173–2179.

[33] Y. Nie, Y. Kimura, T. Inoue, F. Yin, E. Akiyama, K. Tsuzaki, Hydrogen embrittlement of a 1500-MPa tensile strength level steel with an ultrafine elongated grain, Metall. Mater. Trans 43 (5) (2012) 1670–1687.

[34] A.K. Belyaev, V.A. Polyanskiy, Yu.A. Yakovlev, Stresses in pipeline affected by hydrogen, Acta Mech. 3–4 (2012) 176–186.

[35] A. Belyaev, A. Polyanskiy, V. Polyanskiy, Y. Yakovlev, Parametric instability in cyclic loading as the cause of fracture of hydrogenous materials, Mech. Solids 47 (2012) 533–537.

[36] A.K. Belyaev, V.A. Polyanskiy, Y.A. Yakovlev, Hydrogen as an indicator of high-cycle fatigue, Proc. IUTAM (Dyn. Anal. Multibody Syst. Des. Uncertain.) 13 (2015) 138–143.

[37] A.H.S. Bueno, E.D. Moreira, J.A.C.P. Gomes, Evaluation of stress corrosion cracking and hydrogen embrittlement in an API grade steel, Eng. Fail. Anal. 36 (2014) 423–431.